

Similarity Relations for Anisotropic Scattering in Monte Carlo Simulations of Deeply Penetrating Neutral Particles

DOUGLAS R. WYMAN, MICHAEL S. PATTERSON, AND BRIAN C. WILSON

*Department of Medical Physics, Hamilton Regional Cancer Centre,
Hamilton, Ontario, Canada L8V 1C3*

Received September 11, 1987; revised February 12, 1988

Transformations of radiation-matter interaction parameters that result in similar radiation distributions are referred to as similarity relations. A class of similarity relations for monoenergetic, or single energy group, neutral particle transport is derived from fundamental transport considerations. One specific relation, defined as the moments similarity relation, is examined as a biased sampling method for Monte Carlo simulations. The moments similarity relation most effectively reduces computation time for simulations involving deep penetration and highly forward peaked scattering. The method involves substantial reductions in the total scattering cross section that can be employed with greatest accuracy away from sources and boundaries. A specific case study for diffuse transmittance and reflectance in a highly scattering medium is presented to illustrate the method and evaluate its computational effectiveness. © 1989 Academic Press, Inc.

INTRODUCTION

The technique of Monte Carlo particle transport simulation is routinely applied in calculations of the absorption of energy or the spatial or angular distribution of particles traversing an attenuating medium. This technique has a wide scope of applications, including ionizing radiation absorption, shielding, and dosimetry, reactor physics, and atmospheric physics. A comprehensive list of references to the fundamental work in these areas, including both charged and neutral particles, is given by Carter and Cashwell [1].

Recently, reports of Monte Carlo simulations of light transport have appeared in the medical physics literature. These simulations involve imaging [2], the absorption of light energy in tissues [3], or the determination of fundamental interaction parameters [4]. The few published measurements of angular scattering data indicate that visible light scattering in blood and soft tissues is highly forward peaked [4, 5]. Also, interaction mean free paths in tissue are typically 10–100 μm , with scattering dominating absorption [5]. A tissue thickness of several centimetres may thus be hundreds or thousands of mean free paths.

A simulation of light transport in such tissue is therefore prohibitively lengthy for

scoring, with even minimal accuracy, the spatial or angular distribution of the transmitted beam. These transmitted quantities might, for example, be sought in image analyses of breast transillumination [2, 6], or in radiation dosimetry for photodynamic therapy [7-9] or laser surgery [10].

Considerable effort has focussed on developing mathematical techniques to reduce simulation time by reducing the variance in scored quantities. The most generally useful of these biasing techniques are splitting and roulette [1], the exponential transform [11, 12], and biasing either the source or the angular scattering distribution [13, 14]. We have found that no combination of existing biasing techniques is sufficiently powerful to enable accurate scoring of transmitted quantities in media that may be more than hundreds of mean free paths thick.

For such simulations one approach could be to modify the interaction parameters of the medium such that the scored quantities are not significantly altered but the effective mean free path is greatly increased. This can be accomplished by using the exponential transformation or by carefully invoking scattering similarity relations [15]. While the exponential transformation is useful, we have found that for accurate results, its single parameter should generally lie between 0.75 and 1.0, representing typically only a 30% stretch in mean free path.

The use of similarity relations in Monte Carlo simulations is not a conventional biasing technique since similarity relations violate the biasing principle of altering probabilities while conserving expectations of interactions at each point in the medium. Similarity relations are discussed at several points in the books by van de Hulst [15].

In this paper, a class of similarity relations, designed to quicken Monte Carlo simulations involving anisotropic scattering in very thick media, is derived from fundamental neutral particle transport considerations. These relations are assessed in a case typical of light propagation in tissue.

THEORY

In a previous paper [17], we described the replacement of a continuous angular scattering probability density function (PDF) by a discrete PDF, according to the matching of moments. The logic of that replacement technique suggests a more general substitution, in which both the angular scattering PDF and the scattering cross section, Σ_s , are altered through a similarity relation. A fundamental derivation of scattering similarity involves consideration of the angular flux, ψ , at each point in the medium. ψ is a solution of the monoenergetic, or single energy group, neutral particle transport equation, which can be written [18] as

$$\frac{1}{v} \frac{\partial \psi}{\partial t} + \mathbf{\Omega} \cdot \nabla \psi + \Sigma_t(\mathbf{r}) \psi(\mathbf{r}, \mathbf{\Omega}, t) = s(\mathbf{r}, \mathbf{\Omega}, t) + \int_{4\pi} \psi(\mathbf{r}, \mathbf{\Omega}', t) \Sigma_s(\mathbf{r}, \mathbf{\Omega}' \rightarrow \mathbf{\Omega}) d\mathbf{\Omega}'. \quad (1)$$

In Eq. (1), the angular flux and general source term, ψ and s , generally have spatial, angular, and time dependence, \mathbf{r} , Ω , t . The total interaction cross section, $\Sigma_t(\mathbf{r})$, is the sum of the absorption and scattering cross section, $\Sigma_a(\mathbf{r})$ and $\Sigma_s(\mathbf{r})$, while $\Sigma_s(\mathbf{r}, \Omega' \rightarrow \Omega)$ is the angular scattering cross section. The exclusion of energy dependence from Eq. (1) implies either elastic scattering or that the angular flux and interaction cross sections are energy averaged [18].

Denote by μ_0 the cosine of the scattering angle between the incident particle direction, Ω' , and the scattered direction, Ω . Equation (1) can then be rewritten as

$$\frac{1}{v} \frac{\partial \psi}{\partial t} + \Omega \cdot \nabla \psi - s(\mathbf{r}, \Omega, t) + I(\mathbf{r}, \Omega, t) = 0, \quad (2)$$

where

$$I(\mathbf{r}, \Omega, t) = \Sigma_a(\mathbf{r}) \psi(\mathbf{r}, \Omega, t) + \Sigma_s(\mathbf{r}) \left[\psi(\mathbf{r}, \Omega, t) - \int_{4\pi} \psi(\mathbf{r}, \Omega', t) \frac{f(\mathbf{r}, \mu_0)}{2\pi} d\Omega' \right] \quad (3)$$

and $f(\mathbf{r}, \mu_0)$ is the PDF for μ_0 .

Suppressing \mathbf{r} and t dependence for notational convenience only and with no loss in generality, it is clear from Eq. (2) that any Σ_a^* , Σ_s^* , and $f^*(\mu_0)$ can be equivalently substituted for Σ_a , Σ_s , and $f(\mu_0)$ in Eq. (3) provided the quantity $I(\Omega)$ remains invariant. The exact equivalence requirement is thus

$$[(\Sigma_a - \Sigma_a^*) + (\Sigma_s - \Sigma_s^*)] \psi(\Omega) = \int_{4\pi} \frac{\psi(\Omega')}{2\pi} [\Sigma_s f(\mu_0) - \Sigma_s^* f^*(\mu_0)] d\Omega'. \quad (4)$$

To explicitly relate the original and substituted parameters, expand the angular flux and angular scattering PDFs using spherical harmonics and Legendre functions [19], respectively, as follows:

$$\psi(\Omega) = \sum_{n=0}^{\infty} \sum_{m=-n}^n a_{mn} Y_n^m(\theta, \xi) \quad (5)$$

$$f(\mu_0) = \sum_{j=0}^{\infty} \left(\frac{2j+1}{2} \right) f_j P_j(\mu_0) \quad (6)$$

$$f^*(\mu_0) = \sum_{j=0}^{\infty} \left(\frac{2j+1}{2} \right) f_j^* P_j(\mu_0). \quad (7)$$

The expansion coefficients f_j and f_j^* can be formally calculated as Legendre moments of $f(\mu_0)$ and $f^*(\mu_0)$. Substitution of Eqs. (5)–(7) into Eq. (4), and simplification using the addition theorem and orthogonality properties (see Appendix 1) results in the following equivalence requirement:

$$a_{mn} [\Sigma_s(1 - f_n) - \Sigma_s^*(1 - f_n^*) + (\Sigma_a - \Sigma_a^*)] = 0, \quad n \geq 0. \quad (8)$$

Note that a_{00} represents the scalar flux, being ψ integrated over all angles, and it is always positive. Also, $f(\mu_0)$ and $f^*(\mu_0)$ are PDFs so that $f_0 = f_0^* = 1.0$. Using $n = 0$, Eq. (8) thus implies that $\Sigma_a^* = \Sigma_a$ and so no alternate absorption cross section is possible. In a region where $a_{mn} \approx 0$ for $n > N$, the angular flux expansion in Eq. (5) can be terminated at $n = N$. In such a region, the angular flux is N th order anisotropic and the equivalence requirement in Eq. (8) reduces to

$$\frac{\Sigma_s^*}{\Sigma_s} = \frac{1 - f_n}{1 - f_n^*}, \quad n = 1, \dots, N. \quad (9)$$

For each N , Eq. (9) defines a similarity relation. Referring to the class of relations in Eq. (9) as a general moments similarity relation, it is clear that increasing N increases the order of flux anisotropy admitted by, and thus the accuracy of, the moments similarity relation. Unfortunately, this forces Σ_s^* and $f^*(\mu_0)$ to approach Σ_s and $f(\mu_0)$, thereby reducing the computational power of the relation in Monte Carlo simulations. Qualitatively, this moments similarity relation should be applied by using a high order relation near sources or boundaries, where the angular flux is highly anisotropic and a low order relation deep in the medium.

It is shown in Appendix 2 that as $N \rightarrow \infty$, there can be no distinct similarity relation. This proves that, in general, the angular flux corresponds to a unique set of interaction parameters. The N th order moments similarity relation can be employed, however, with accuracy limited by the assumption that the angular flux is at most N th order anisotropic.

The following factors should be considered when selecting Σ_s^* and $f^*(\mu_0)$ that obey the moments similarity relation:

(1) The similarity ratio, S , defined as the ratio Σ_s^*/Σ_s , must lie between 0 and 1 and be as small as possible for a given N , in order to maximally reduce simulation time. S is the factor by which the moments similarity relation stretches the scattering mean free path;

(2) $f^*(\mu_0)$ must be positive for all $\mu_0 \in (-1, 1)$ and simple in form so that it can be quickly randomly sampled;

(3) as discussed above, S should generally increase towards unity as N increases. High accuracy (large N) and high speed (small S) cannot be maintained simultaneously. If attempted, negative values of $f^*(\mu_0)$ will result;

(4) it should be possible to calculate S given only the coefficients f_n , to allow easy assessment of the power of the relation prior to its application in a simulation.

Of the obvious choices for functional forms of $f^*(\mu_0)$ (step, linear, quadratic, Dirac delta spikes), the following step function satisfies the first three conditions and optimally satisfies the fourth condition. Denote the j th of the $n-1$ local extrema of the n th Legendre function, $P_n(x)$, by x_{jn} and the abscissa endpoints at

-1 and 1 by x_{0n} and x_{nn} , respectively. Next, select as the amplitude of the j th of n steps between -1 and 1,

$$W_{jn}(x) = \begin{cases} (x_{jn} - x_{j-1,n})^{-1}, & x \in (x_{j-1,n}, x_{jn}) \\ 0, & \text{otherwise.} \end{cases} \quad (10)$$

Then construct $f^*(\mu_0)$ for the N th-order similarity relation from $W_{jN}(\mu_0)$ as follows:

$$f^*(\mu_0) = \sum_{j=1}^N a_j W_{jN}(\mu_0), \quad (11)$$

The first few functions W_{jn} are given in Fig. 1. The following properties make the W_{jn} useful as components of $f^*(\mu_0)$:

$$W_{jn}(x) = W_{n+1-j,n}(x), \quad n > 0 \quad (12a)$$

$$\int_{-1}^1 W_{jn}(x) dx = 1, \quad n > 0 \quad (12b)$$

$$\int_{-1}^1 W_{jn}(x) P_n(x) dx = 0, \quad n > 0 \quad (12c)$$

$$\int_{-1}^1 W_{jn}(x) W_{in}(x) dx = \delta_{ij}/(x_{jn} - x_{j-1,n}), \quad n > 0 \quad (12d)$$

In particular, property (12c) ensures compliance with the second and fourth conditions for $f^*(\mu_0)$ since it renders $f_N^* = 0$ and so

$$S = 1 - f_N. \quad (13)$$

The functions $W_{jn}(x)$ can be referred to as orthogonal block functions and the scattering transformation in Eq. (13) is hereafter referred to as the moments similarity relation. It can be shown, using Eqs. (7), (9), and (11), that the N coefficients a_j can be calculated by solving the $N \times N$ linear algebraic system

$$\sum_{j=1}^N a_j L_{jn} = \frac{S-1+f_n}{S}, \quad n = 0, \dots, N-1, \quad (14)$$

where

$$L_{jn} = \int_{-1}^1 W_{jN}(x) P_n(x) dx. \quad (15)$$

For $N \leq 4$, Eq. (14) is easily solved algebraically.

The moments similarity relation, Eq. (13), is most useful when N is large, such as generally arises from highly forward-peaked scattering. When $f_N = 0$, as in isotropic scattering, the moments similarity relation is useless.

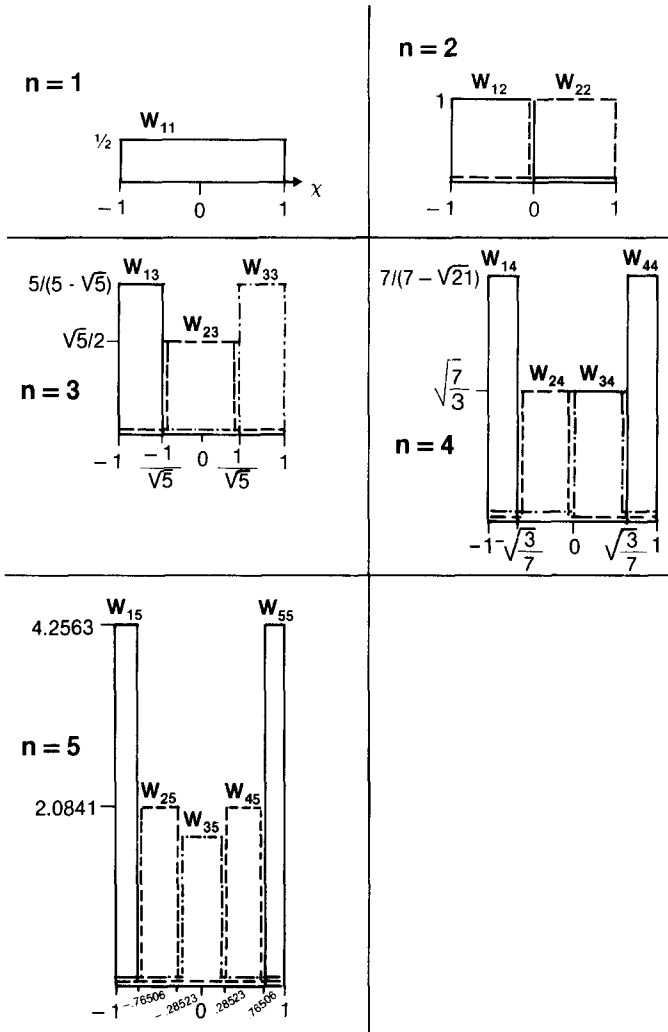


FIG. 1. The orthogonal block functions, $W_{j\mu}(x)$.

CASE STUDY

The expected reduction in computation time using the moments similarity relation can be demonstrated as follows. Suppose that for an infinite homogeneous slab of thickness M mean free paths, as in Fig. 2, one employs the actual angular scattering PDF in the first M_{entrance} mean free paths and in the final M_{exit} mean free paths, where higher flux anisotropy occurs. By using the moments similarity

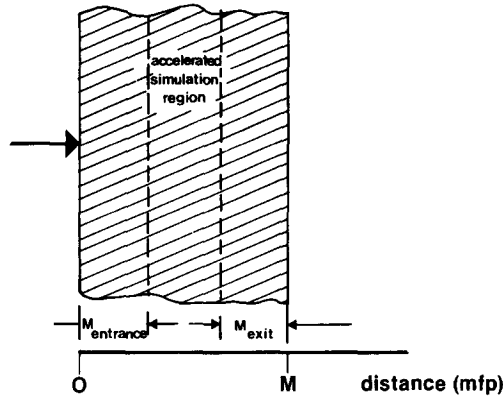


FIG. 2. Infinite homogeneous test slab of thickness M mean free paths, with variable angular scattering PDF, $\alpha = 0.99$ and for which the moments similarity relation accelerates the simulation in the central region.

relation with similarity ratio, S , at all remaining interior points, the computation time should be reduced at least by the factor

$$r = \left[S + (1 - S) \left(\frac{M_{\text{entrance}} + M_{\text{exit}}}{M} \right) \right]^{-1} \quad (16)$$

As expected, $r \rightarrow 1$ as $S \rightarrow 1$. The time reduction factor should actually exceed r , since the moments similarity relation projects particles well into the entrance and exit regions before a switch to the actual angular scattering PDF can be made. As an example, for $\bar{\mu}_0 = 0.98$ with M_{entrance} , M_{exit} , and M of 100, 50, and 2000 mean free paths, the $N = 1$ moments similarity relation would reduce computation time by a factor exceeding 10.7.

The method of scattering equivalence embodied in Eqs. (11) and (13) was first tested by simulating the transport of neutral particles normally incident on an infinite homogeneous test slab, Fig. 2, with thicknesses M_{entrance} , M_{exit} , and M of 10, 10, and 30 mean free paths. The simulations were conducted using the standard techniques of Monte Carlo simulation, including non-absorption weighting [1], with no other variance reduction techniques. While homogeneous, the slab is divided into three regions. The actual angular scattering PDF, valid for all three regions but used only in the first and third regions, is a Henyey–Greenstein function [15], with the following functional form:

$$f_{\text{HG}}(\mu_0) = 0.5(1 - \bar{\mu}_0^2)(1 + \bar{\mu}_0^2 - 2\bar{\mu}_0\mu_0)^{-3/2}. \quad (17)$$

This smooth PDF is characterized by a single parameter, $\bar{\mu}_0$, governing anisotropy, and has the useful property that f_n is $\bar{\mu}_0^n$.

The simulation was accelerated only in the central region by sampling using the moments similarity relation, consisting of the equivalent angular scattering PDF,

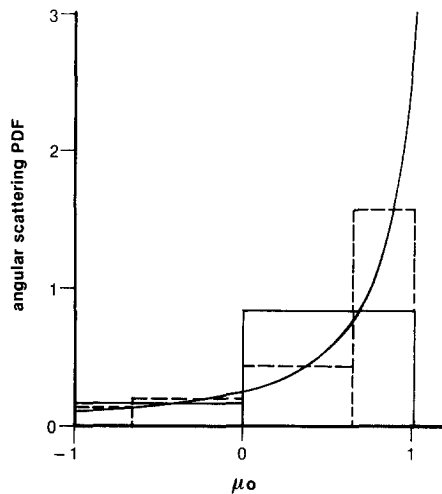


FIG. 3. Henyey–Greenstein continuous angular scattering PDF with $\bar{\mu}_0 = 0.5$, and corresponding orthogonal block functions for $N = 2$ (solid square) and $N = 4$ (dashed square).

$f^*(\mu_0)$, and scattering cross section, Σ_s^* . The actual and replacement angular scattering PDFs, for $\bar{\mu}_0 = 0.5$, are shown in Fig. 3. The total diffuse transmittance, T , and diffuse reflectance, R , were scored for varying scattering anisotropy, central region thickness, and N , the order of equivalence. The single scattering albedo, α , is defined as the fraction, Σ_s/Σ_t , of interactions that are scatters. For this test, a high albedo of $\alpha = 0.99$ was used since a high albedo normally applies in deep penetration calculations.

The results are presented in Fig. 4 as a comparison of computed R and T values with corresponding correct values, calculated by simulation using the actual angular scattering PDF. The correct values for $\bar{\mu}_0 = 0.5$ are $T = 0.0151$, $R = 0.6628$ and for $\bar{\mu}_0 = 0.9$ are $T = 0.1828$, $R = 0.3806$. All observed deviations are quoted as a relative error arising from inherent inaccuracy of the scattering equivalence. Reflected particles were also scored with spatial discrimination for the above test slab with $\bar{\mu}_0 = 0.5$, $\alpha = 0.99$, and $N = 2$. This test allows assessment of the moments similarity relation for scoring accuracy of distributed quantities. The results, containing negligible statistical error, are presented in Fig. 5.

A simulation was also conducted to verify the computational savings afforded by the moments similarity relation. The simulation involved normal incidence on an infinite homogeneous slab of thickness 100 mean free paths, characterized by $\alpha = 1.0$ and a Henyey–Greenstein PDF with $\bar{\mu}_0 = 0.9$. For this case, Eq. (16) predicts a time reduction factor exceeding 2.84 when the moments similarity relation of order $N = 2$ ($R = 0.19$) is used in the central 80 mean free paths. The actual time reduction factor in the simulation was 4.0.

Finally, simulations were conducted to check the accuracy of the moments

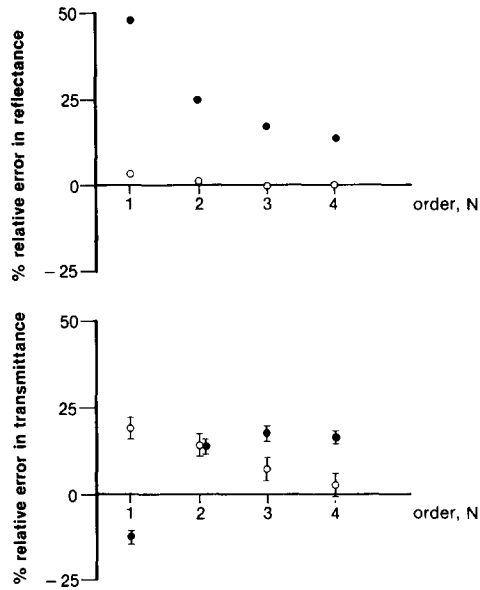


FIG. 4. Relative error in transmittance (T) and reflectance (R) for simulations involving normal incidence on the test slab of Fig. 2, with thicknesses M_{entrance} , M_{exit} and M of 10, 10, and 30 mean free paths, and for different orders, N , in the moments similarity relation. The actual angular scattering PDF is a Henyey–Greenstein function with $\bar{\mu}_0 = 0.5$ (open circles) and $\bar{\mu}_0 = 0.9$ (solid circles). The error bars represent statistical simulation error.

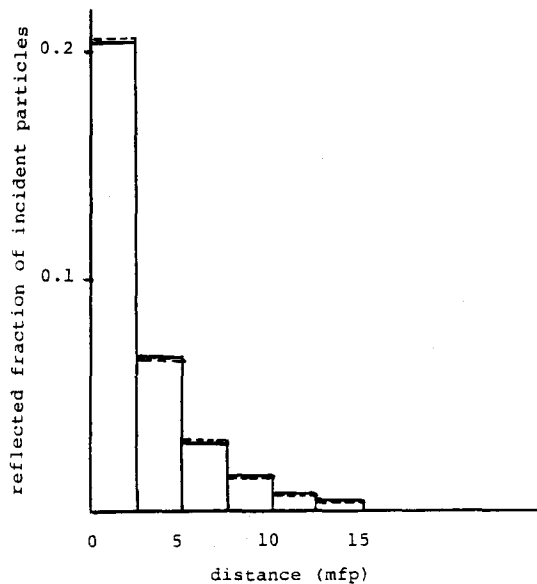


FIG. 5. Total diffusely reflected particles scored as a function of distance, on the test slab face, from a line source normally incident on the test slab used to generate Fig. 4, with $\bar{\mu}_0 = 0.5$: using moments similarity relation ($N=2$) (solid lines); correct values (dashed lines).

TABLE I

Transmittance (T) and reflectance (R) from simulation of normal incidence on thick infinite homogeneous slabs with $\alpha = 1.0$ and a Henyey-Greenstein angular scattering PDF with $\bar{\mu}_0 = 0.9$.

Slab thickness (mean free paths)	Using moments similarity relation			Correct values		
	T	R	Time	T	R	Time
100	($N = 2$) 0.112 ± 0.002	0.888 ± 0.002	0.41	0.143 ± 0.004	0.857 ± 0.004	1.0
150	($N = 2$) 0.075 ± 0.002	0.925 ± 0.002	0.39	0.100 ± 0.001	0.900 ± 0.001	1.0
150	($N = 3$) 0.085 ± 0.002	0.915 ± 0.002	0.42	0.100 ± 0.001	0.900 ± 0.001	1.0
150	($N = 4$) 0.094 ± 0.002	0.906 ± 0.002	0.49	0.100 ± 0.001	0.900 ± 0.001	1.0

similarity relation in problems of deep penetration, typically characterized by a high albedo with highly forward peaked scattering involving many mean free paths of penetration. The simulations were conducted for normal incidence on infinite homogeneous slabs of thickness 100 and 150 mean free paths, each with $\alpha = 1.0$ and a Henyey-Greenstein angular scattering PDF with $\bar{\mu}_0 = 0.9$. The moments similarity relation was used between 20 and 80 mean free paths into the narrower slab and between 30 and 130 mean free paths into the thicker slab. Since no published data could be found for such deep penetration, the correct values were obtained through Monte Carlo simulation without the moments similarity relation and thus have associated statistical errors. The results are presented in Table I.

DISCUSSION

Inspection of Fig. 4 confirms that scoring accuracy increases with the order, N , of the moments similarity relation. For a given entrance region, in which the actual angular scattering PDF is used, scoring accuracy increases as $\bar{\mu}_0$ decreases. It follows from the results in Fig. 4, for example, that the 10 mean free path entrance region of the test slab in Fig. 2 is sufficient if the moments similarity relation with $N = 2$ replaces a Henyey-Greenstein angular scattering PDF with $\bar{\mu}_0 = 0.5$. A thicker entrance region is required if $\bar{\mu}_0$ is increased to 0.9 since, in that case, the flux anisotropy at 10 mean free paths depth substantially exceeds second order. As suggested by the high accuracy obtainable when scoring reflected particles both totally, Fig. 4, and with spatial discrimination, Fig. 5, the moments similarity relation can accurately reproduce both integral and distributed quantities.

In general, accuracy using the moments similarity relation is acquired by expanding the entrance and exit regions in which unbiased sampling is performed, at the expense of computation time. For a given accuracy, the required thickness of the entrance and exit regions varies approximately inversely with the similarity ratio, S . This variation implies, as suggested by the results in Table I, that when $\bar{\mu}_0$ exceeds 0.9, either thick entrance regions and central regions with low order relations, or

thin entrance regions and central regions with high order relations, may be required. However the simulation is conducted in the entrance and exit regions, maximal reduction of computation time in deep penetration simulations is achieved by using a low order relation in the vast central region.

In practice, the user should perform a prior narrow slab simulation to ensure an adequate entrance region for a subsequent lengthy thick slab simulation. The exit region thickness can usually be set equal to the entrance region thickness, since flux anisotropy would usually be greatest in the entrance region.

The computational savings afforded by the moments similarity relation depends uniquely on the N th Legendre moment of the actual angular scattering PDF. The relation is most effective for highly forward peaked scattering, generally characteristic of deep penetration problems.

The moments similarity relation is easily compared with the existing similarity relations presented by van de Hulst [15]. Based on a matching of diffusion exponents and with the caution that similarity relations cannot be trusted to yield accurate results, van de Hulst suggests that similarity is generally best achieved by maintaining invariant the quantity

$$q = \frac{1 - \alpha}{1 - \alpha\bar{\mu}_0}. \quad (18)$$

This can be achieved by varying any of the three fundamental parameters Σ_a , Σ_s , $\bar{\mu}_0$. In particular, by leaving Σ_a constant while switching to isotropic scattering ($\bar{\mu}_0 \rightarrow 0$), Eq. (18) reduces to the first-order moments similarity relation ($N=1$). Equation (18) is therefore valid only when the angular flux is approximately linearly anisotropic, defined as the diffusion region. As indicated by Table I, for nearly conservative and highly forward peaked scattering, similarity relations more accurate than Eq. (18) should be used in simulations near the surface.

Finally, the moments similarity relation should be applied cautiously in simulations involving heterogeneities or irregular geometry, since highly anisotropic fluxes are normally found near material boundaries. A high order relation should therefore be used near boundaries and, as for the entrance region, a prior simulation in simplified slab geometry can suggest minimum distances inside which the scattering interaction should be sampled exactly. Indeed, similarity relations may be useless in cases where multiple heterogeneities are closely spaced.

SUMMARY

The problem of finding valid similarity relations between the various fundamental interaction parameters that determine neutral particle transport has been solved in this work through considerations of transport equation invariance. A general class of similarity relations has been derived based on the result that in a region of N th order flux anisotropy, exact similarity can be achieved by suitably transform-

ing the first $N + 1$ Legendre moments of the angular scattering distribution. Extending from this derivation is a proof that a general angular flux with arbitrary anisotropy can result from at most one set of physically plausible interaction parameters. A particular class of these relations, defined here as the moments similarity relation, has been suggested and examined because of its simplicity and usefulness in expediting Monte Carlo simulations. Existing similarity relations correspond to a first-order moments similarity relation.

The moments similarity relation most effectively reduces computation time for simulations in very thick media involving highly forward peaked scattering. Computation time reductions can be predicted prior to simulation and can easily exceed a factor of 10.

It is anticipated that an important application of the moments similarity relation will involve simulating the transport of red and infrared light through living tissues, since these conditions involve optically thick media with high albedo and highly forward peaked scattering.

APPENDIX 1: DERIVATION OF EQ. (8)

The equivalence requirement in Eq. (8) is derived from Eq. (4) using Eqs. (5)–(7). By the addition theorem [19], $f(\mu_0)$ and $f^*(\mu_0)$ are expanded as

$$\begin{aligned} f(\mu_0) &= 2\pi \sum_{j=0}^{\infty} \sum_{l=-j}^j f_j Y_j^l(\theta, \xi) \bar{Y}_j^l(\theta', \xi') \\ f^*(\mu_0) &= 2\pi \sum_{j=0}^{\infty} \sum_{l=-j}^j f_j^* Y_j^l(\theta, \xi) \bar{Y}_j^l(\theta', \xi'), \end{aligned} \quad (\text{A1})$$

where the bar superscript denotes complex conjugation. Substituting the expansions in Eqs. (A1) and (5) into Eq. (4) yields

$$\begin{aligned} &\sum_{n=0}^{\infty} \sum_{m=-n}^n [(\Sigma_a - \Sigma_a^*) + (\Sigma_s - \Sigma_s^*)] a_{mn} Y_n^m(\theta, \xi) \\ &= \sum_{n=0}^{\infty} \sum_{m=-n}^n \sum_{j=0}^{\infty} \sum_{l=-j}^j [\Sigma_s f_j - \Sigma_s^* f_j^*] a_{mn} Y_j^l(\theta, \xi) \\ &\quad \times \int_0^{\pi} \int_0^{2\pi} Y_n^m(\theta', \xi') \bar{Y}_j^l(\theta', \xi') \sin(\theta') d\xi' d\theta'. \end{aligned} \quad (\text{A2})$$

By orthogonality [19], the double integral in Eq. (A2) is just $\delta_{nj} \delta_{ml}$ so that Eq. (A2) reduces to

$$\sum_{n=0}^{\infty} \sum_{m=-n}^n [(\Sigma_a - \Sigma_a^*) + (\Sigma_s - \Sigma_s^*) - (\Sigma_s f_n - \Sigma_s^* f_n^*)] a_{mn} Y_n^m(\theta, \xi) = 0. \quad (\text{A3})$$

Again by orthogonality, Eq. (A3) implies

$$a_{mn}[\Sigma_s(1-f_n) - \Sigma_s^*(1-f_n^*) + (\Sigma_a - \Sigma_a^*)] = 0 \quad (\text{A4})$$

which is Eq. (8) in the text.

APPENDIX 2

THEOREM. *An angular flux, ψ , being a solution of the neutral particle transport equation, Eq. (1), can result from at most one set of physically plausible interaction parameters, Σ_a , Σ_s , $f(\mu_0)$.*

Proof. (Spatial and time dependence have been notationally suppressed without mathematical loss of generality). Assume that Σ_a^* , Σ_s^* , and $f^*(\mu_0)$ yield the same angular flux, ψ , as a given set of parameters Σ_a , Σ_s , and $f(\mu_0)$. In general, ψ has an unlimited order of anisotropy. Equations (8) and (9) show that the parameters must be related by

$$\Sigma_a^* = \Sigma_a \quad (\text{A5})$$

$$\Sigma_s^* = \Sigma_s \left[\frac{1-f_n}{1-f_n^*} \right], \quad n \geq 1, \quad (\text{A6})$$

where f_n and f_n^* are Legendre expansion coefficients for $f(\mu_0)$ and $f^*(\mu_0)$. Substituting f_n^* from Eq. (A6) into the Legendre expansion for $f^*(\mu_0)$, Eq. (7), results in

$$\begin{aligned} f^*(\mu_0) &= \sum_{j=0}^{\infty} \left(\frac{2j+1}{2} \right) \left[\left(1 - \frac{\Sigma_s}{\Sigma_s^*} \right) + \left(\frac{\Sigma_s}{\Sigma_s^*} \right) f_j \right] P_j(\mu_0) \\ &= \left(1 - \frac{\Sigma_s}{\Sigma_s^*} \right) \delta(\mu_0 - 1) + \left(\frac{\Sigma_s}{\Sigma_s^*} \right) f(\mu_0). \end{aligned} \quad (\text{A7})$$

To be physically plausible, $f^*(\mu_0)$ must be nonnegative, implying, Eq. (A7), that $\Sigma_s^* \geq \Sigma_s$. Furthermore, if scattering is governed by Σ_s^* and $f^*(\mu_0)$, Eq. (A7) shows that only the fraction Σ_s/Σ_s^* of scatters under $f^*(\mu_0)$ occur at angles other than 0, effectively changing Σ_s^* to Σ_s in any calculation. Thus, practically, $\Sigma_s^* = \Sigma_s$, and so $f^*(\mu_0) = f(\mu_0)$, completing the proof. Alternatively, Eq. (A7) may be viewed as a trivial similarity relation of no practical utility.

REFERENCES

1. L. L. CARTER AND E. D. CASHWELL, *Particle-Transport Simulation with the Monte Carlo Method* (U.S. Energy Research Development Administration, Washington, DC, 1975).
2. J. M. MAAREK, G. JARRY, J. CROWE, M. H. BUI, AND D. LAURENT, *Med. Biol. Eng. Comput.* **24**, 407 (1986).

3. B. C. WILSON AND G. ADAM, *Med. Phys.* **10**, 824 (1983).
4. P. A. WILKSCH, F. JACKA, AND A. J. BLAKE, in *Porphyrin Localization and Treatment of Tumors*, edited by D. R. Doiron and C. J. Gomer (Alan R. Liss, 1984), p. 149.
5. S. T. FLOCK, B. C. WILSON, AND M. S. PATTERSON, *Med. Phys.* **14**, 835 (1987).
6. S. ERTEFAI AND A. E. PROFIO, *Med. Phys.* **12**, 393 (1985).
7. B. C. WILSON AND M. S. PATTERSON, *Phys. Med. Biol.* **31**, 327 (1986).
8. L. I. GROSSWEINER, *Lasers Surg. Med.* **6**, 462 (1986).
9. S. L. JACQUES AND S. A. PRAHL, *Lasers Surg. Med.* **6**, 494 (1987).
10. TH. HALLDORSSON, W. ROTHER, J. LANGERHOLC, AND F. FRANK, *Lasers Surg. Med.* **1**, 253 (1981).
11. L. B. LEVITT, *Nucl. Sci. Eng.* **31**, 500 (1968).
12. M. LEIMDORFER, *Nukleonik* **6**, 58 (1964).
13. C. E. BURGART AND F. N. STEVENS, *Nucl. Sci. Eng.* **42**, 306 (1970).
14. J. M. LANORE, *Nucl. Sci. Eng.* **45**, 66 (1971).
15. H. C. VAN DE HULST, *Multiple Light Scattering*, Vol. 2 (Academic Press, New York, 1980).
16. H. C. VAN DE HULST AND K. GROSSMAN, in *The Atmospheres of Venus and Mars* (Gordon & Breach, New York, 1968).
17. D. R. WYMAN AND M. S. PATTERSON, *J. Comput. Phys.* **76**, 414 (1988).
18. J. J. DUDERSTADT AND L. J. HAMILTON, *Nuclear Reactor Analysis* (Wiley, New York, 1976).
19. G. B. ARFKEN, *Mathematical Methods for Physicists* (Academic Press, New York, 1970).